

Co-catalyst free Titanate Nanorods for improved Hydrogen production under solar light irradiation

N LAKSHMANA REDDY, D PRAVEEN KUMAR and M V SHANKAR*

Nanocatalysis and Solar Fuels Research Laboratory, Department of Materials Science and Nanotechnology, Yogi Vemana University, Vemanapuram, Kadapa 516 003, Andhra Pradesh, India
e-mail: shankar@yogivemanauniversity.ac.in

MS received 14 December 2015; revised 1 February 2016; accepted 17 February 2016

Abstract. Harnessing solar energy for water splitting into hydrogen (H_2) and oxygen (O_2) gases in the presence of semiconductor catalyst is one of the most promising and cleaner methods of chemical fuel (H_2) production. Herein, we report a simplified method for the preparation of photo-active titanate nanorods catalyst and explore the key role of calcination temperature and time period in improving catalytic properties. Both as-synthesized and calcined material showed rod-like shape and trititanate structure as evidenced from crystal structure and morphology analysis. Notably, calcination process affected both length and diameter of the nanorods into shorter and smaller size respectively. In turn, they significantly influenced the band gap reduction, resulting in visible light absorption at optimized calcination conditions. The calcined nanorods showed shift in optical absorption band edge towards longer wave length than pristine nanorods. The rate of hydrogen generation using different photocatalysts was measured by suspending trititanate nanorods (in the absence of co-catalyst) in glycerol-water mixture under solar light irradiation. Among the catalysts, nanorods calcined at 250°C for 2 hours recorded high rate of H_2 production and stability confirmed for five cycles. Photocatalytic properties and plausible pathway responsible for improved H_2 production are discussed in detail.

Keywords. Water splitting; hydrogen production; photocatalysis; glycerol; nanorods

1. Introduction

Industrial and domestic activities have severely damaged the earth eco-system and the present situation warranted technology up-gradation and innovative developments for sustainable future. Intensive research has been carried out in alternative energy sector to replace fast depleting non-renewable fossil fuels. Hydrogen (H_2) production *via* photocatalytic water splitting process is reported as the best alternative and renewable source of H_2 production and emits eco-friendly by-products e.g., oxygen.^{1–5} Use of natural resources, like solar light and water paves the way for sustainable development. Among the photocatalysts developed for H_2 production by water splitting, TiO_2 based, one dimensional (1-D) nanostructures are of greater interest due to their interesting opto-electrical properties, unidirectional flow of electrons due to electron confinement which is advantageous for photocatalytic applications.^{6–9} In 1-D TiO_2 nanostructures, the trititanate nanorod (TNR) attracts much attention owing to their higher stability, better crystallinity and presence of long axis to absorb incident light enabling nanorods as suitable candidate for photocatalytic water splitting and dye

sensitized solar cells (DSSCs) applications.^{10–13} Literature reports revealed that performance of photocatalysts was highly influenced by several factors such as crystal structure, particle size, particle shape, method of synthesis and post synthesis calcination process.^{14,15} Hydrothermal method is known as simple and eco-friendly method widely used for synthesis of 1-D nanostructures of TiO_2 as it shows high yield at low temperature.^{16–18} The activity of photocatalyst was influenced by experimental parameters like presence of co-catalyst, reaction temperature and duration, solution pH, type of hole scavengers, nature of salt, etc. In addition, post-synthesis process like calcination temperature and duration improves the crystallinity of the TiO_2 nanorods which in turn influence the activity of the photocatalysts.¹⁵ We have been developing several TiO_2 materials and their nanocomposite photocatalysts demonstrated high activity for H_2 production under solar light irradiation.^{19–24} Based on our expertise in synthesis and application of Ti-O based nanostructures, they were suitably functionalized for efficient water purification in mixed matrix membranes,²⁵ an excellent solid-acid catalyst for rapid synthesis of one-pot multi-component synthesis^{26,27} and a novel approach to nanotherapy for autoimmune diseases.²⁸

*For correspondence

In the present work, cheap and non-photoactive commercial TiO_2 was used as the starting material for synthesis of lab-scale, photoactive titanate nanorods (TNR). They were frequently used to study photocatalytic decontamination of organic pollutants in water with some noble metal or metal oxide co-catalyst.^{14,29–32} But to the best of our knowledge, only a few reports exist on unmodified and co-catalyst-free trititanate nanostructures for H_2 production. For example, Liu *et al.*, demonstrated photocatalytic H_2 evolution ($220 \mu\text{mol} \cdot \text{h}^{-1} \cdot \text{g}_{\text{cat}}^{-1}$) using commercial biphasic anatase-rutile TiO_2 nanopowder without use of co-catalyst.³³ Another report revealed the open circuit H_2 production from black TiO_2 nanotubes ($7 \mu\text{mol} \cdot \text{h}^{-1} \cdot \text{g}_{\text{cat}}^{-1}$).³⁴ Chuangchote and co-workers explained synthesis of electrospun TiO_2 nanofibers and tested its performance for photocatalytic H_2 evolution ($54 \mu\text{mol} \cdot \text{h}^{-1} \cdot \text{g}_{\text{cat}}^{-1}$).³⁵ The present study exploits the effect of calcination temperature and time period to improve H_2 production using glycerol as sacrificial hole scavenger in the absence of any co-catalysts.

2. Experimental

2.1 Synthesis of Titanate nanorods

All the chemicals used for the present work are of analytical grade. Titanate nanorods were synthesized by hydrothermal method with slight modifications to the earlier report.¹⁰ In a typical process 4 g of commercial TiO_2 (Merck-LAB, India) was suspended in 200 mL of 10 M NaOH solution and magnetically stirred for 1 h. The obtained milk-white slurry was transferred into 250 mL capacity stainless steel autoclave and sealed for hydrothermal treatment at 200°C for 24 h. Then, autoclave was allowed for natural cooling, and obtained precipitate was thoroughly washed with dilute HCl, distilled water and ethanol, followed by drying at 80°C for 12 h. The obtained nanorods were calcined at different calcination temperature for time period of 1, 2 and 3 h in order to study the effect of post heat treatment on photocatalytic activity. The details of the photocatalysts and its nomenclature are presented below.

2.2 Photocatalyst Characterization Techniques

All the prepared materials were thoroughly characterized with different characterization techniques. XRD pattern was obtained by Bruker D8 Advance X-ray - diffractometer using $\text{Cu K}\alpha$ radiation ($\lambda = 1.54\text{\AA}$). Raman spectra were recorded with Raman spectrometer (LABRAM HR) operating with an excitation wavelength of 632 nm and power of 1 mW. The TEM images were taken with Philips Technai G2 FEI F12 transmission electron microscope operating at 80-100 kV. Optical properties were measured in DRS – UV-Vis spectrophotometer (Varian Cary-5000).

2.3 Solar photocatalytic experiments

Photocatalytic experiments were conducted under solar light irradiation in sunny days between 10.00 AM and 3.00 PM. In a typical process, 5 mg of catalyst was suspended in 5% glycerol-water mixture (50 mL) in 150 mL capacity Quartz reactor and was allowed for magnetic stirring for adsorption of glycerol and water molecules for 30 min, followed by evacuation and nitrogen purging for 30 min of each step to remove gases and to simulate inert atmosphere for reduction reaction. Then, the Quartz reactor was kept under solar light irradiation for the photocatalytic H_2 production *via* water splitting. Generated gas samples were tested at regular intervals of time using Gas Chromatograph (SHIMADZU GC-2014) with thermal conductivity detector (TCD) and molecular sieve-5A by injecting the gas sample with 250 μL capacity syringe.

3. Results and Discussion

3.1 Characterization of Photocatalysts

The TEM images of TNR and TNR-2 are depicted in figure 1(a-c). It reveals that overlapping of several rod-like shapes and its diameter is in the nanoscale.¹⁰ TNR and TNR-2 look like cylindrical in shape filled inside, very smooth and clean without any other contamination. Length of the TNR is about 1- 4 μm and

Photocatalyst	Nomenclature
As synthesized Titanate Nanorods	TNR
Titanate Nanorods calcined @ $200^\circ\text{C}/2\text{h}$	TNR-1
Titanate Nanorods calcined @ $250^\circ\text{C}/1\text{h}$	TNR-2-1
Titanate Nanorods calcined @ $250^\circ\text{C}/2\text{h}$	TNR-2
Titanate Nanorods calcined @ $250^\circ\text{C}/3\text{h}$	TNR-2-3
Titanate Nanorods calcined @ $300^\circ\text{C}/2\text{h}$	TNR-3
Titanate Nanorods calcined @ $400^\circ\text{C}/2\text{h}$	TNR-4

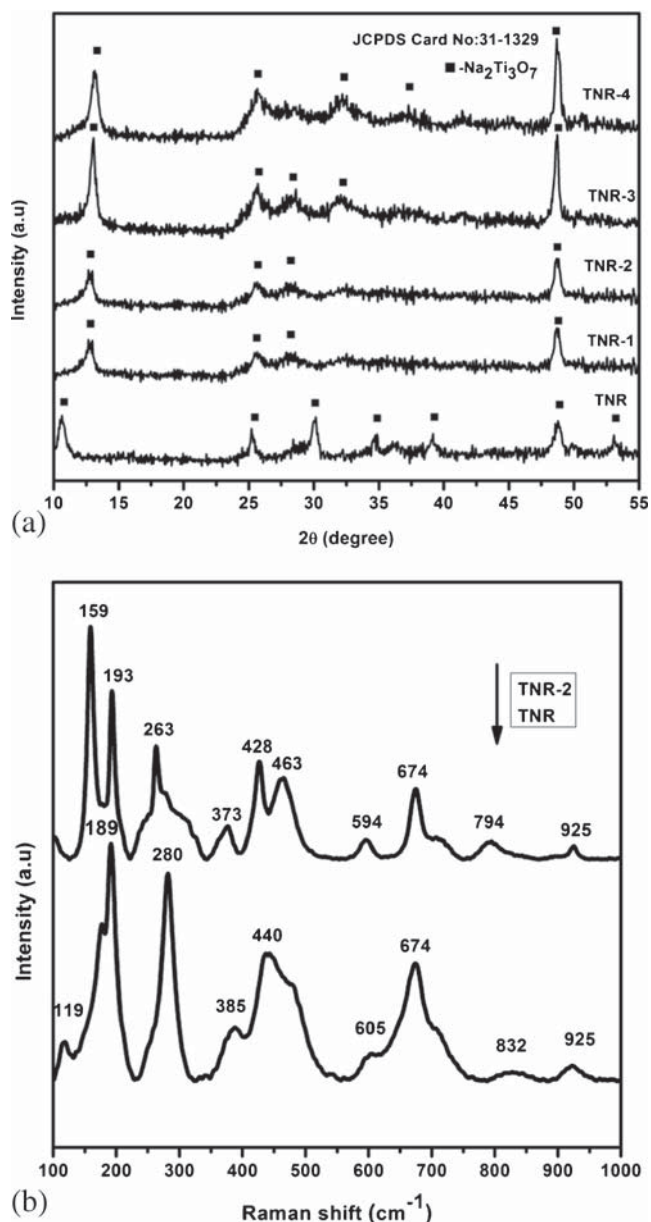


Figure 2. (a) XRD pattern of as-synthesized and calcined TNR. (b) Raman spectrum of as-synthesized and calcined TNR.

appeared for TNR at 119, 280, 440, 674 and 925 cm^{-1} and for TNR-2, the observed shifts at 159, 193, 373, 428, 463, 674, and 925 cm^{-1} reveal $\text{Na}_2\text{Ti}_3\text{O}_7$ with monoclinic structure. These data are in accordance with earlier reports.^{10,39} Particularly, the band at 280 cm^{-1} for TNR corresponds to Na-O-Ti stretching vibrations⁴⁰ and the bands at 159 and 193 cm^{-1} of TNR-2 corresponds to Na-O-Ti bending modes⁴³ and it clearly demonstrates that formed nanostructure is $\text{Na}_2\text{Ti}_3\text{O}_7$. For TNR and TNR-2, we can find that most peaks related to Ti-O based structure are almost the same. It demonstrates that it does not undergo structural changes. Minor absorption shift in bands of TNR

at 189 and 440 cm^{-1} showed doublets at 159, 193 and 428, 463 cm^{-1} , respectively, after thermal treatments, and the changes indicate that calcined nanorods showed phase shift as evidenced by XRD results. For TNR and TNR-2, the relative intensities varied. The band at 674 cm^{-1} for TNR-2 represented Ti-O-Ti stretching vibration in edge-shared TiO_6 octahedral.⁴⁰ The changes in the relative intensities of TNR and TNR-2 are caused by dehydration of water molecules in the lattice structures during thermal treatment and these observations are in tune with the XRD results.

Optical properties of the titanate nanorods were examined using DRS-UV-Vis spectrophotometer. The absorption spectra (figure 3(a)) revealed that with respect to calcination temperature the characteristics of absorption by nanorods (TNR-2: 385 nm, TNR-3: 388 nm, TNR-4: 391 nm, TNR: 364 nm) showed red shift. The band gap values for all the photocatalysts were calculated by using Kubelka-Munk function by plotting

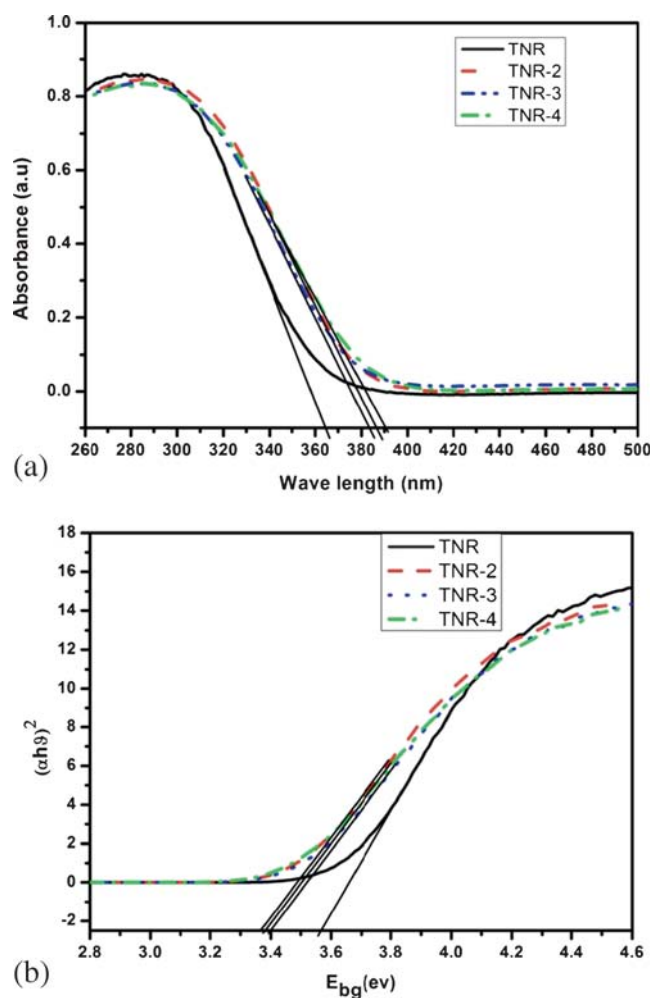


Figure 3. (a) DR UV-Vis spectra TNR catalysts; (b) Plot of transformed Kubelka-Munk function $(\alpha h\nu)^2$ vs. photon energy ($h\nu$, eV) for as-synthesized and calcined TNR catalysts to estimate band gap energies by linear extrapolation.

a graph between $(\alpha h\nu)^2$ vs. photon energy ($h\nu$) and the plot is shown in figure 3(b). Decrease in band gap value from 3.58 to 3.33 eV for TNR and TNR-4, respectively, was noted and similar changes were reported in literature.^{39,41} The relative decrease in band gap of the calcined titanate nanorods strongly affected surface and optical properties.³⁶ The red shift in absorption is attributed to improvement of crystallinity *via* de-hydroxylation of surface hydroxyl groups and desorption of physisorbed water molecules which result in shorter and smaller size of nanorods.

3.2 Photocatalytic hydrogen production

The photocatalytic activity of the prepared Titanate nanorods was tested under direct solar light irradiation for 4 h. Figure 4(a) displays the effect of calcination temperature (from 200 to 400°C) on the rate of photocatalytic H₂ production. It is evident that TNR-2 (calcined at 250°C) showed the highest rate of H₂

production of 707 $\mu\text{mol} \cdot \text{h}^{-1} \cdot \text{g}_{\text{cat}}^{-1}$ in aqueous glycerol solution. The high catalytic activity as mentioned above is attributed to one dimensional flow of photogenerated charge carriers and facile electron donating nature of glycerol facilitated effective oxidation and reduction reactions. The lower catalytic activity is recorded for TNR-1 photocatalyst and is assigned to lower catalytic active sites, whereas low activity of TNR-3 and TNR-4 catalysts is assigned to limited availability of photogenerated charge carriers at catalyst surface for the reaction. In this study, at lower catalyst calcination temperature, the poor crystallinity noticed in X-ray diffraction pattern, is a result of fewer active sites available for the catalytic reaction. Moreover, temperature above optimal calcination tends to form particle-particle agglomeration of catalyst and diminished the surface area and active sites of the catalyst.⁴⁵ Yoshida *et al.*,³⁷ explained that experimental parameters like calcination temperature and time strongly influence the efficiency of the photocatalyst. Recent reports emphasized that the calcination temperature significantly affects the crystallinity and alter the shape of the catalytic material.^{36,42}

The prepared TNRs were calcined at different calcination duration *viz.*, 250°C/1 h, 250°C/2 h and 250°C/3 h denoted as TNR-2-1, TNR-2 and TNR-2-3, respectively, to study the effect of calcination time. Figure 4(b), shows the TNR calcined at different calcination time versus photocatalytic H₂ production. In comparison, TNR-2 showed improved H₂ production than other catalysts. The TNR-2-1 showed lower activity due to lower crystallinity and whereas the lower activity for TNR-2-3 is due to agglomeration of the nanostructures at longer duration of calcination.

Recyclability tests were performed for the optimized photocatalyst (TNR-2) for 5 cycles under solar light irradiation in order to estimate the stability of the photocatalyst (figure 5). In each cycle, TNR-2 was irradiated for 4 h, the generated gas samples were quantified

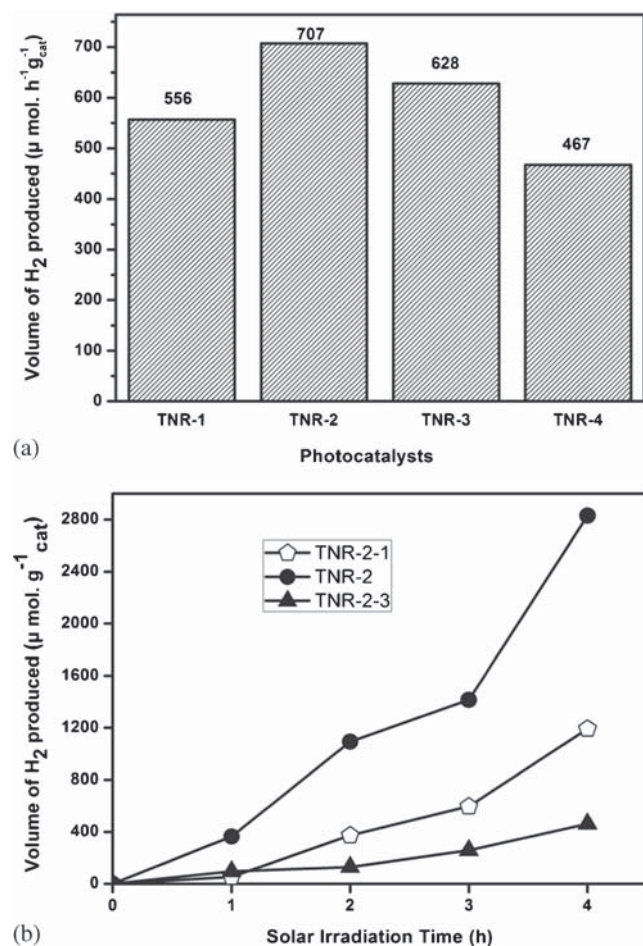


Figure 4. (a). Effect of calcination temperature for photocatalytic H₂ production in aqueous glycerol solution under solar light irradiation. (b). Effect of calcination duration for photocatalytic H₂ production in aqueous glycerol solution under solar light irradiation.

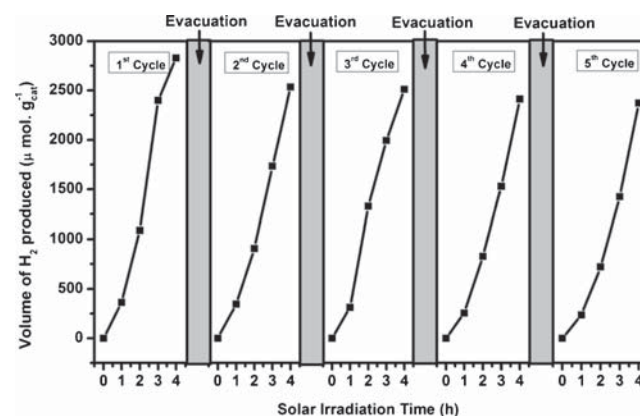


Figure 5. Recyclability of TNR-2 under solar irradiation.

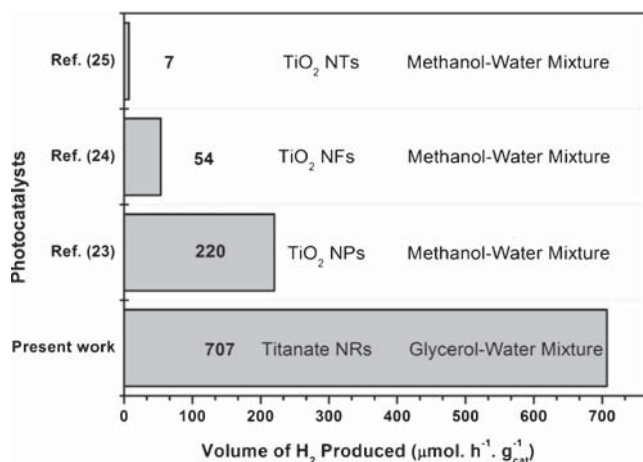


Figure 6. Comparison of solar H₂ generation using TiO₂ photocatalysts.

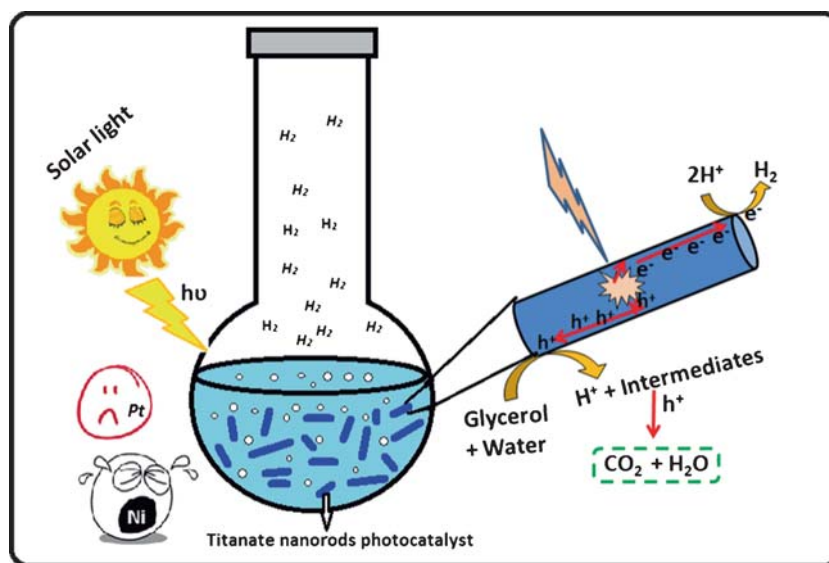
for each hour using Gas Chromatograph equipped with TCD. After 1st cycle, the quartz reactor was evacuated to eliminate gases and purged with N₂ gas for inert atmosphere and again irradiated by solar light for 2nd cycle, and the evolved gases were again tested using gas chromatograph similar to 1st cycle. The same procedure was followed for 3rd, 4th and 5th cycle of experiments. In all the cycles, stable H₂ generation was seen. About 83.8% of H₂ generated at 5th cycle. In 4th and 5th cycles, the H₂ generation was slightly less, which may be due to decomposition of sacrificial agent (glycerol), and increase in the number of intermediate products in glycerol reforming process.⁴⁶ These recyclability experiments reveal that our prepared titanate nanorod photocatalyst has exhibited very good stability for longer hours.

Recent reports on photocatalytic H₂ generation using TiO₂ nanoparticles and nanostructures without co-catalyst in presence of sacrificial reagents have been compared with the present work. Here, we used industrial byproduct glycerol as sacrificial reagent whereas others have used methanol. Figure 6 shows the photocatalytic H₂ production of TiO₂ nanorod-based photocatalysts. The high activity is ascribed to shape of nanorods and electron donating nature glycerol present in the aqueous solution.

Based on the experimental results, a plausible reaction mechanism is proposed. The beneficial properties of the 1-D nanostructures, such as catalytic active sites available on the surface, uni-directional flow of electrons along the axis of the nanorods, minimization of electron-hole pairs are shown in scheme 1. When solar light irradiates the titanate nanorods, the valence band (VB) electrons get excited and transferred to the conduction band (CB) and migrate to the surface of the 1-D nanorods and holes remain in the VB. First, oxidation reaction takes place with holes on VB and forms H⁺ ions from either water or glycerol, and these H⁺ ions undergo reduction to H₂ with photogenerated electrons at CB of nanorods. Alternatively, holes in VB oxidize glycerol and its intermediates into H⁺ ions. These intermediates produce H⁺ ions, and CO₂ under prolonged light irradiation.

4. Conclusions

In summary, post-synthesis calcination process significantly improved the photocatalytic activity of sodium titanate nanorods prepared using hydrothermal



Scheme 1. Proposed reaction mechanism of titanate nanorods for photocatalytic H₂ production under direct solar light irradiation.

method. Structural analysis revealed that trititanate nanorods have layered structure and interlayer distance decreases with optimized calcination temperature and time period, which is ascribed to dehydration of water molecules. The examination of optical properties and morphology of titanate nanorods with calcination shows shift in band edge and decrease in length of nanorods. The solar photocatalytic performance studied in batch mode under ambient conditions and nitrogen atmosphere showed that the rate of hydrogen production was influenced by both calcination temperature and time period. The TNRs calcined at 250°C for 2 h (TNR-2) showed improved activity ascribed to synergetic functions of 1-D nanostructure, stable morphology with thermal treatments and minimal defect sites that lead to fast transfer of charge carriers to the surface for improved photocatalytic hydrogen generation. In the present study, the improved H₂ production rate is ascribed for two major reasons: (i) One dimensional titanate nanorods catalyst effectively delocalized the photogenerated charge carriers (electron-hole) along its length but confined the movement in exterior walls of nanorods. (ii) The improved adsorption and electron donating nature of glycerol served as suitable hole scavenger for continuous production of H⁺ ions. The present study highlighted that post-synthesis heat treatment can improve the photocatalytic performance in the absence of any co-catalyst. Moreover, the recyclability tests demonstrated the stability of the photocatalyst for 5 cycles without any significant loss in its catalytic performance. The experimental results demonstrated that glycerol undergoes photocatalytic reforming and produces H⁺ ions instantaneously which undergoes reduction with photogenerated electrons for H₂ production.

Acknowledgements

N. Lakshmana Reddy is grateful to Department of Science and Technology (DST), New Delhi [IF 131053] for financial support through INSPIRE Fellowship.

References

- Liao C H, Huang C W and Wu J C S 2012 *Catalysts* **2** 490
- Chen X, Shen S, Guo L and Mao S S 2010 *Chem. Rev.* **110** 6503
- Rajaambal S, Sivaranjani K and Gopinath C S 2015 *J. Chem. Sci.* **127** 33
- Daya Mani A, Xanthopoulos N, Laub D and Subrahmanyam, C H 2014 *J. Chem. Sci.* **126** 967
- Tijare S N, Bakardjieva S, Subrt J, Joshi M V, Rayalu S S, Hishita S and Labhsetwar N 2014 *J. Chem. Sci.* **126** 517
- Wang X, Li Z, Shi J and Yu Y 2014 *Chem. Rev.* **114** 9346
- Lee K, Mazare A and Schmuki P 2014 *Chem. Rev.* **114** 9385
- Zhou W, Liu H, Boughton R I, Du G, Lin J, Wang J and Liu D 2010 *J. Mater. Chem.* **20** 5993
- Ma Y, Wang X, Jia Y, Chen X, Han H and Li C 2014 *Chem. Rev.* **114** 9987
- Kolenko Y V, Kovnir K A, Gavrilov A I, Garshev A V, Frantti J, Lebedev O I, Churagulov B R, Van Tendeloo O G and Yoshimura M 2006 *J. Phys. Chem. B* **110** 4030
- Lee E, Hong J Y, Kang H and Jang J 2012 *J. Hazard. Mater.* **219** 13
- Khemthong P, Photai P and Grisdanurak N 2013 *Int. J. Hydrogen Energy* **38** 15992
- Yan K, Wu G, Jarvis C, Wen J and Chen A 2014 *Appl. Cat. B: Environ.* **148** 281
- Yun H J, Lee H, Joo J B, Kim N D and Yi J 2011 *J. Nanosci. Nanotechnol.* **11** 1
- Huang C W, Liao C H and Wu J C S 2013 *J. Clean Energy Technol.* **1** 1
- Hayashi H and Hakuta Y 2010 *Materials* **3** 3794
- Natarajan S, Mandal S, Mahata P, Koteswara Rao V, Ramaswamy P, Banerjee A, Kumar Paul A and Ramya K V 2006 *J. Chem. Sci.* **118** 525
- Byrappa K and Adschiri T 2007 *Prog. Cryst. Growth. Charact. Mater.* **53** 117
- Praveen Kumar D, Shankar M V, Mamatha Kumari M, Sadanandam G, Srinivas B and Durga Kumari V 2013 *Chem. Commun.* **49** 9443
- Praveen Kumar D, Lakshmana Reddy N, Mamatha Kumari M, Srinivas B, Durga Kumari V and Shankar M V 2014 *JoCC* **1** 13
- Praveen Kumar D, Shankar M V, Lakshmana Reddy N, Parasuramudu D, Rajarajeswari D and Durga Kumari V 2013 *Solar Light Active CuO/TiO₂ Nanobelt Photocatalyst for Enhanced H₂ Production*, Proceedings of the "International Conference on Advanced Nanomaterials & Emerging Engineering Technologies" organized by Sathyabama University, Chennai, India in association with DRDO, New Delhi, India. 24th–26th July 2013.
- Praveen Kumar D, Lakshmana Reddy N, Srinivas B, Durgakumari V, Roddatis V, Bondarchuk O, Karthik M, Ikuma Y and Shankar M V 2016 *Sol. Energy Mater. Sol. Cells* **146** 63
- Praveen Kumar D, Lakshmana Reddy N, Mamatha Kumari M, Srinivas B, Durgakumari V, Roddatis V, Bondarchuk O, Karthik M, Nepplian B and Shankar M V 2015 *Sol. Energy Mater. Sol. Cells* **136** 157
- Mamatha Kumari M, Praveen Kumar D, Haridoss P, Durga Kumari V and Shankar M V 2015 *Int. J. Hydrogen Energy* **40** 1665
- Sumisha S, Arthanareeswaran G, Ismail A F, Praveen Kumar D and Shankar M V 2015 *RSC Adv* **49** 39464
- Rajendra Prasad Reddy B, Vasu Govardhana Reddy P, Praveen Kumar D, Reddy B N and Shankar M V 2016 *RSC Adv.* **6** 14682
- Rajendra Prasad Reddy B, Venkata Krishna Reddy M, Vasu Govardhana Reddy P, Praveen Kumar D and Shankar M V 2016 *Tetrahedron Lett.* **51** 696
- Sree Latha T, Dakshayani L, Praveen Kumar D, Shankar M V and Madhava Reddy C 2016 *RSC Adv.* **6** 8870
- Pu Y C, Chen Y C and Hsu Y J 2010 *Appl. Cat. B: Environ.* **97** 389

30. Sun T, Fan J, Liu E, Liu L, Wang Y, Dai H, Yang Y, Hou W, Hu X and Jiang Z 2012 *Powder Technol.* **228** 210
31. Khan M A, Akhtar M S, Woo S I and Yang O B 2008 *Catal. Commun.* **10** 1
32. Liu C, Tang J, Chen H M, Liu B and Yang P 2013 *Nano Lett.* **13** 2989
33. Liu N, Schneider C, Freitag D, Venkatesan U, Reddy M V R, Hartmann M, Winter B, Spiecker E, Osvet A, Zolnhofer E M, Meyer K, Nakajima T, Zhou X and Schmuki P 2014 *Angew. Chem. Int. Ed.* **53** 14201
34. Liu N, Schneider C, Freitag D., Hartmann M, Venkatesan, U, Muller J, Spiecker E and Schmuki P 2014 *Nano Lett.* **14** 3309
35. Chuangchote S, Jitputti J, Sagawa T and Yoshikawa S 2009 *ACS Appl. Mater. Interfaces* **1** 1140
36. Morgado E, Abreu M A S, Pravia O R C, Marinkovic B A, Jardim P M, Rizzo F C and Araujo A S 2006 *Solid State Sci.* **8** 888
37. Yoshida R, Suzuki Y and Yoshikawa S J 2005 *Solid State Chem.* **178** 2179
38. Papp S, Korosi L, Meynen V, Cool P, Vansant E F and Dekany I 2005 *J. Solid State Chem.* **178** 1614
39. Wu Z, Guo S, Wang H and Liu Y 2009 *Electrochem. Commun.* **11** 1692
40. Menga X, Wang D, Liu J and Zhang S 2004 *Mater. Res. Bull.* **39** 2163
41. Fu X, Leung D Y C and Chen S 2014 *Cryst. Eng. Comm.* **16** 616
42. Kiatkittipong K, Iwase A, Scott J and Amal R 2013 *Chem. Eng. Sci.* **93** 341
43. Ren N, Li R, Chen L, Wang G, Liu D, Wang Y, Zheng L, Tang W, Yu X, Jiang H, Liu H and Wu N 2012 *J. Mater. Chem.* **22** 19151
44. Zhu G N, Wang C X and Xia Y Y 2011 *J. Power Sources* **196** 2848
45. Vijayan B, Dimitrijevic N M, Rajh T and Gray K 2010 *J. Phys. Chem. C* **114** 12994
46. Bowker M, James D, Stone P, Bennett R, Perkins N, Millard L, Greaves J and Dickinson A 2003 *J. Catal.* **217** 133